Journal of the Korean Ceramic Society
Vol. 51, No. 1, pp. 1~6, 2014.

http://dx.doi.org/10.4191/kcers.2014.51.1.001

Facile Preparation of Ag_2S-CNT Nanocomposites with Enhanced Photo-catalytic Activity

Ze-Da Meng*,*, Sourav Sarkar**, Lei Zhu**, Kefayat Ullah**, Shu Ye**, and Won-Chun Oh**,†**

*Jiangsu Key Laboratory of Environmental Functional Materials, College of Chemistry and Bioengineering, Suzhou University of Science and Technology, Suzhou 215009, China

**Department of Advanced Materials Science & Engineering, Hanseo University, Seosan-si 356-706, Korea

(Received September 2, 2013; Revised December 2, 2013; Accepted January 7, 2014)

ABSTRACT

Here we report improved photo-catalytic effect of Ag_2S under visible light using carbon nano-tubes (CNT) modified with Ag_2S nanoparticles. The optical properties, structural properties and compositional analysis, as well as the photo-electrochemical properties of the prepared composites were investigated. It was found that the photocurrent density, and the photo-catalytic effect, was increased by modification of CNT in this way. Compared with the separate effects of Ag_2S and CNT nanoparticles, the photo-catalytic effect of CNT-modified-with-Ag_2S composites, increased significantly due to a synergistic effect between the CNT and the Ag_2S nanoparticles.

Key words : CNT, Ag_2S, Visible light, FTIR, UV-vis, TBA

1. Introduction

In recent years, nano-sized semiconductors have been studied extensively due to their technological importance.[1)] With the development of photoelectric detection technology, semiconducting photoelectric detectors of high efficiency and accuracy have been applied abroad. Based on their regions of photoelectric response, detectors are distinguished as ultraviolet, visible light and infrared photoelectric-detectors. Currently, silicon is at the core of visible light photoelectric detectors; possessing excellent photoelectric properties in the region of visible light.[2,3)]

Silver sulfide has attracted considerable attention because of its potential for uses in optoelectronic and thermoelectric materials; such as photovoltaic cells, photoconductors, IR detectors and super-ionic conductors.[4)] Ag_2S nanoparticles with different morphologies have been prepared by various methods, including the gamma-ray irradiation reduction route, aminopoly-carboxylic acids-capped method, hydrothermal routeand solvo-thermal process, among others. However, it still remains a challenge to develop an easier fabrication process for Ag_2S nanoparticles so as to extend its applications (e.g., electrochemical DNA detection analysis).[5)]

Carbon nanotube (CNT)-based composites has received great attention due to the fact that their conductivity can be increased significantly with a relatively low concentration of carbon in the host material.[6)] Moreover, multi wall carbon nanotubes (MWCNTs) have a variety of interesting electronic properties. In one of their possible electronic structures, they may exhibit metallic conductivity. MWCNTs have a large electron-storage capacity (one electron per 32 carbon atoms), and the properties of MWCNTs can promote the electron-transfer reactions in carbon-nanotube-modified materials.[7)] There are reports that the separation of photo-generated charge carriers is more efficient in the hetero-junctions of $TiO_2$and CNTs. In photo-electrochemical cells it was observed that the photosensitivity increased with the use of TiO_2/CNT composites.[8)] The principal effect of CNT was to increase the absorption of UV light and enhance electron transport at the CNT/TiO_2photo-anode.[9)]

In this work, we prepared Ag_2S-CNT nanoparticles by the sonochemistry method.These nanoparticles combine the excellent charge-transport property of Ag_2S and the absorption property of CNT. These catalysts were irradiated with visible light and their catalytic activities compared.

2. Experimental Procedure

2.1. Materials

Benzene (99.5%) and ethyl alcohol were purchased as reagent-grade from Duksan Pure Chemical Co. (Korea) and Daejung Chemical Co. (Korea); then used as received. Crystalline CNT powder (diameter: 20 nm, length: 5 μm) of 95.9 wt% purity from Carbon Nano-material Technology Co. , Ltd., Korea, was used as one of the carbon nanomaterials. Silver nitrate ($AgNO_3$) and sodium sulfide·5-hydrate ($Na_2S·5H_2O$) were supplied by Duksan Pure Chemical Co., Ltd, Korea. Texbrite BA-L (TBA) was purchased from Texchem Co. Ltd, Korea. All chemicals were used without fur-

†Corresponding author : Won-Chun Oh
E-mail : wc_oh@hanseo.ac.kr
Tel : +82-41-660-1337 Fax : +82-41-688-3352

ther purification, and all experiments were carried out using distilled water.

2.2. Preparation of Ag_2S particles

The Ag_2S nanoparticles were prepared via a precipitation process using $AgNO_3$ and $Na_2S{\cdot}5H_2O$ as precursors. First, 1.02 g of $AgNO_3$was dissolved in 100 mL of distilled water, and then 0.003 mol of $Na_2S{\cdot}5H_2O$ solution was added dropwise into the above solution with sonication at room temperature for 30 min. Then, the mixture was vigorously stirred and subjected to ultrasonication for 6 h. For purification, the mixture was rinsed and centrifuged several times with acetone and distilled water. After filtration and drying under vacuum at 80°C, Ag_2S was obtained as a black powder.

2.3. Oxidation of CNT surface

MCPBA (m-chloroperbenzoic acid, ~1 g) was suspended in 50 ml of benzene, followed by the addition of CNT (~0.5 g). The mixture was then refluxed in an air atmosphere and stirred for 6 h. The solvent was subsequently dried at the boiling point of benzene (353.13 K). After completion, the dark brown precipitates were washed with ethyl alcohol and dried at 323 K, after which the oxidized CNT was formed.

2.4. Preparation of Ag_2S-CNT particles

A stoichiometric amount of 30 ml of $AgNO_3$ solution was mixed with oxidized CNT. With continuous stirring at 343 K, 50 ml of Na_2S aqueous solution was then added to the mixture drop-by-drop; at the rate of 6 drops/min. After ultra sonication for 7 h, the final mixture was then filtered and washed with deionized water. Through heat treatment at 573 K for 1 h, the dark green Ag_2S-CNT powder was obtained.

2.5. Characterization of Ag_2S-CNT compounds

For the measurement of structural variation, XRD patterns were taken using an X-ray generator (Shimadzu XD-D1, Japan) with Cu Ká radiation. SEM was used to observe the surface state and structure of Ag_2S-CNT composites using a scanning electron microscope (JSM-5200 JOEL, Japan). Energy dispersive X-ray (EDX) spectroscopy was also used for elemental analysis of the samples. The Brunauer–Emmett–Teller (BET) surface area was determined by N_2 adsorption measurements at 77 K (Monosorb, USA). Transmission electron microscopy (TEM, JEOL, JEM-2010, Japan) was used to observe the surface state and structure of the Ag_2S-CNT composites. At the acceleration voltage of 200 kV, TEM was used to investigate the size and distribution of the titanium and iron particles deposited on the CNT surfaces in various samples. TEM specimens were prepared by placing a few drops of the sample solution on a carbon grid.

2.6. Catalytic degradation of TBA

Photo-catalytic activity was evaluated by dye degradation in aqueous media under visible-light irradiation. For visible-light irradiation, the reaction beaker was located axially and held in a visible-light lamp box (8 W, halogen lamp, KLD-08L/P/N, Korea). The luminous efficacy of the lamp was 80 lm/W, and the wavelength ranged from 400 - 790 nm. The lamp was located at a distance of 100 mm from the aqueous solution in a dark box. The amount of photo-catalytic composite used was 0.05 g per 50 ml solution. On the other hand, 0.001 v/v aqueous solution of TBA was also prepared with deionized water in 1 L measuring flasks. The concentrations of the stock solutions of the three dyes depended on various factors such as color intensity of the dyes, complexity of molecular structure, intensity of visible light falling on the solutions and activity of the photo-catalysts.

The reactor was placed for two hours in the dark box to allow the photo-catalytic composite particles to adsorb as many dye molecules as possible. After the adsorption phase, visible-light irradiation was restarted to make the degradation reaction proceed. To perform dye degradation, a glass reactor (diameter : 4 cm, height : 6 cm) was used, and the reactor was placed on the magnetic churn dasher. The suspension was then irradiated with visible light for a set irradiation time. Visible-light irradiation of the reactor was performed for 90 min. Samples were withdrawn regularly from the reactor, and dispersed powders were removed in a centrifuge. The clean, transparent solution was analyzed using a UV-vis spectrophotometer (Optizen POP, Mecasys Co., Ltd., Korea). The dye concentration in the solution was determined as a function of the irradiation time.

2.7. Circle use for Ag_2S-CNT composites

The used Ag_2S-CNT composites were immersed in ethanol for 6 h, rinsed with deionized water, and then dried at 353 K. After this, the cleaned Ag_2S-CNT composites were reused to remove dyes, and the experimental cycle was done several times.

3. Results and Discussion

3.1. Surface characteristics of the samples

The micro-surface structures and morphologies of the three different Ag_2S-CNT composites were characterized using SEM. Figure1 shows the macroscopic changes in the morphology of the composites. Ag_2S is shown to have a small particle size and good dispersion. We conjecture that the spherical particles in Ag_2S-CNT composites are Ag_2S particles on the surface of CNT clusters. HRTEM was able to reveal clearly the presence of Ag_2S particles on the surface of CNTs. Zhang et al. reported that a good dispersion of small particles could provide more reactive sites for the reactants than aggregated particles.[10] At the same time, the conductivity of CNT can facilitate electron transfer between the adsorbed dye molecules and the catalyst substrate. By comparing Fig. 1(a) with 1(b) (after adding CNT), the dispersion of Ag_2S was a little deteriorated.

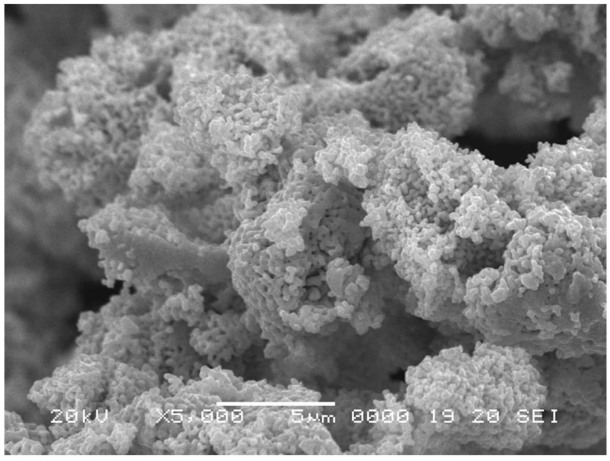

(a)

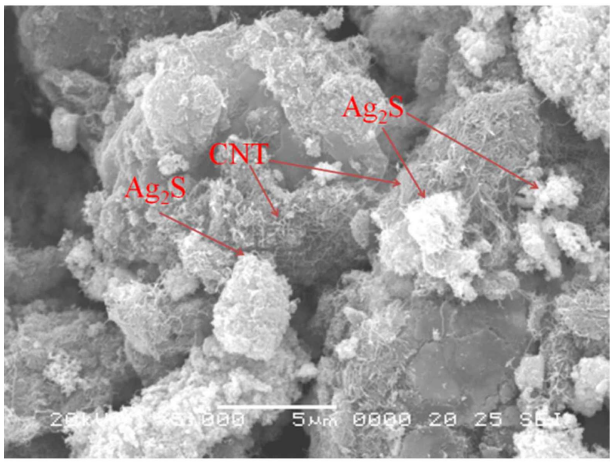

(b)

Fig. 1. SEM images of composites: (a) Ag_2S and (b) Ag_2S-CNT.

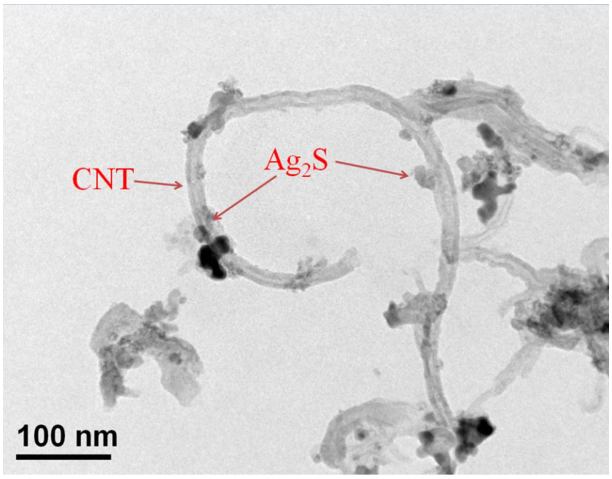

Fig. 2. TEM image of Ag_2S-CNT photocatalyst.

Figure 2 shows HRTEM images of the Ag_2S-CNT composites at different magnifications. HRTEM is a technique used for analyzing the morphology, crystallographic structure, and even the composition of a specimen. Figure 2 gives

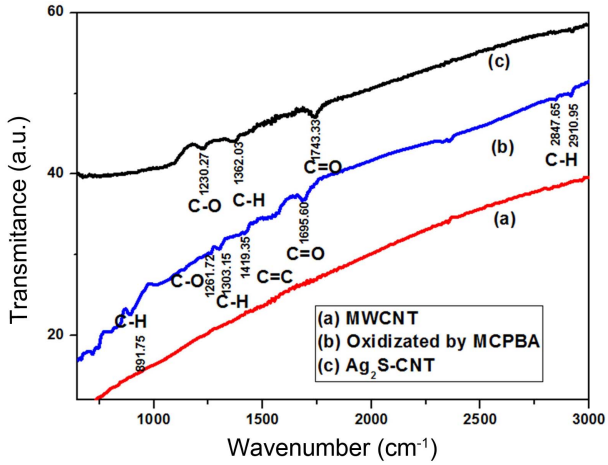

Fig. 3. FT-IR spectra of CNT, oxidation CNT, and Ag_2S-CNT composite.

direct evidence that the CNTs are in close contact with Ag_2S, and particles were observed upon enlargement of the image. This indicates that the surfaces of the Ag_2S particles are cleaned under exposure to the reaction conditions. Ag_2S particles were distributed on the surfaces of CNTs with a size of approximately 20 nm, even though this caused partial agglomeration to form block particles.

3.2. Structural features of the catalyst

FT-IR was conducted on as-received CNTs. Functionalized CNTs and their corresponding spectra are shown in Fig. 3. For the as-received CNTs, the IR spectra showed almost no functional groups on the surface. However, after being oxidized by MCPBA, the MWCNTs had various kinds of functional groups on the surface. The band at 2,910 cm^{-1} and 2,847 cm^{-1} was ascribed to C-H stretching vibration; while the bands at 1,695 cm^{-1}, 1303 cm^{-1}, and 2,847 cm^{-1} were ascribed to C = O, C-H, and C-H stretching vibration, respectively.[11] The above observations suggest that oxidation was promoted in all treatments, and that the functional groups formed, could increase the active sites on the surface of CNTs. Moreover, in the spectra of as-received MWCNTs and functionalized CNTs, some small absorption bands around 1410 cm^{-1} exist which were ascribed to C = C stretching vibration. There was another peak at 2,350 cm^{-1} which might have been due to ambient CO_2 in the spectrometer.[12]

Comparing the spectrum curves (Figs. 3(b) and (c)), it can be seen that the peak intensity of the functional group on oxidized CNT was weaker and decreased. This was because some of the functional groups had combined with Ag_2S particles. The Ag_2S particles were bound to CNTs by a variety of functional groups.[13]

XRD was used to determine the crystallographic structure of the inorganic component of the composite. Figure 4 shows the XRD patterns of the Ag_2S-CNT samples. The main sharp peaks, which were assigned to (111), (112), (121),

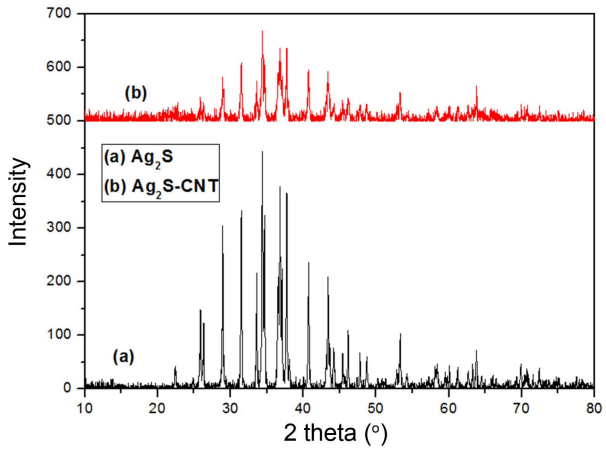

Fig. 4. XRD patterns of composites.

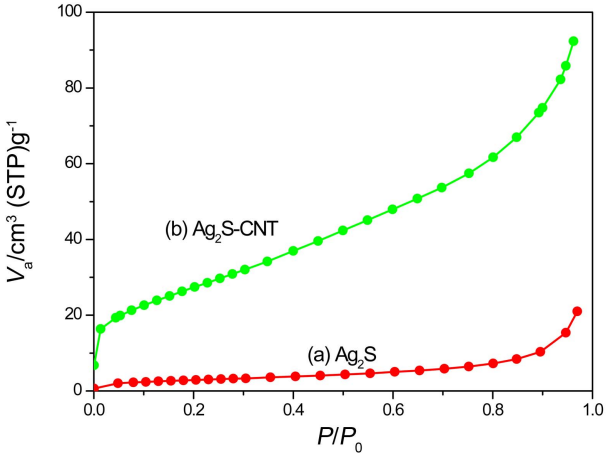

Fig. 5. N_2 adsorption isotherms for (a) Ag_2S and (b) Ag_2S-CNT.

(103), (031), (200), (213), and (134) crystal planes; originate from the acanthite Ag_2S phase.[14] In the XRD pattern of Ag_2S- CNT (Curve b), CNT peaks cannot be found because of the small content of CNT. From the XRD patterns, it is also possible to compute the % crystallinity and crystal size. The amorphous-phase fraction of the sample may be determined using the ratio of the amorphous area (area not under the peaks) of the X-ray diffractogram to the total area. Also, the peaks at different crystal planes of the Ag_2S-CNT nanocomposite, matched exactly with that of Ag_2S, indicating essentially no difference with respect to the type of crystalline phase in the two products. It was found that Ag_2S showed more crystallinity than the prepared Ag_2S-CNT nanocomposite. This is attributed to the adverse conditions created when adding CNT ; which did not allow nucleation and crystal growth to occur fully.[15]

Nitrogen adsorption isotherms for the Ag_2S and Ag_2S-CNT composites are shown in Fig. 5. The formation of Type IV adsorption isotherms confirmed the major presence of mesopores on the surfaces of samples. Characteristic features of the Type IV isotherm are its hysteresis loop, which is associated with capillary condensation taking place in

Table 1. BET Surface Area of the Samples

Sample name	S_{BET} (m^2/g)
Ag_2S	15.95
CNT	169.28
Ag_2S-CNT	63.26

mesopores, and the limiting uptake over a range of high p/p°. The initial part of the Type IV isotherm is attributed to monolayer-multilayer adsorption. This is because it follows the same path as the corresponding part of a Type II isotherm, obtained with the given adsorptive on the same surface area of the adsorbent; in a non-porous form. Type IV isotherms are exhibited by many mesoporous industrial adsorbents.[16,17] This indicates that the Ag_2S and Ag_2S-CNT composites studied were mainly mesoporous in character, with a minor presence of wider pores where capillary condensation occurred. All of the isotherm shapes show similar types for all samples. The BET surface-area values of samples were shown in Table 1. The BET value of Ag_2S-CNT increased from 15.95 m^2/g (CNT only) to 63.26 m^2/g. The Ag_2S-CNT had the largest area; which can affect the adsorption reaction. Surface areas and pore volumes of the Ag_2S-CNT were greater than pure Ag_2S.

3.3. Photo-catalytic activity of samples

Figure 6 shows the time series of TBA degradation using Ag_2S and Ag_2S-CNT composites under irradiation by visible light. The spectra for the TBA solution after visible-light irradiation show the relative degradation yields at different irradiation durations. The decrease in dye concentration continued with a gentle, opposite slope; which was due to visible light irradiation. Two steps are involved in the photo-catalytic decomposition of dyes: the adsorption of dye molecules and degradation. After adsorption in the dark for 30 min, the samples reached adsorption-desorption equilibrium. In the adsorptive step, Ag_2S and Ag_2S-CNT composites showed different adsorptive effects; with Ag_2S-CNT having the best effect. The adsorptive effect of pure Ag_2S was the lowest. The adsorptive effect of Ag_2S-CNT was better than that of Ag_2S because the added carbon materials could enhance the BET surface area; which could increase the adsorption effect. Ag_2S-CNTalso has the largest BET surface area, which can enhance the adsorptive effect. A comparison of the de-coloration effect of the catalysts showed that the degradation effect can be increased by an increase in the adsorption capacity. Fig. 6 represents the degradation of TBA, with Ag_2S and Ag_2S-CNT in visible light; from which it is clear that the concentration of TBA gradually diminished with increasing time; for all samples. The decreasing concentration of TBA in the photo-catalytic reaction was used to evaluate the activity of Ag_2S and Ag_2S-CNT composites. The spectra of the dye solution show the relative degradation yields at different time intervals. Moreover, the dye solution increasingly lost its color intensity as the dye concentration continued to decrease. The

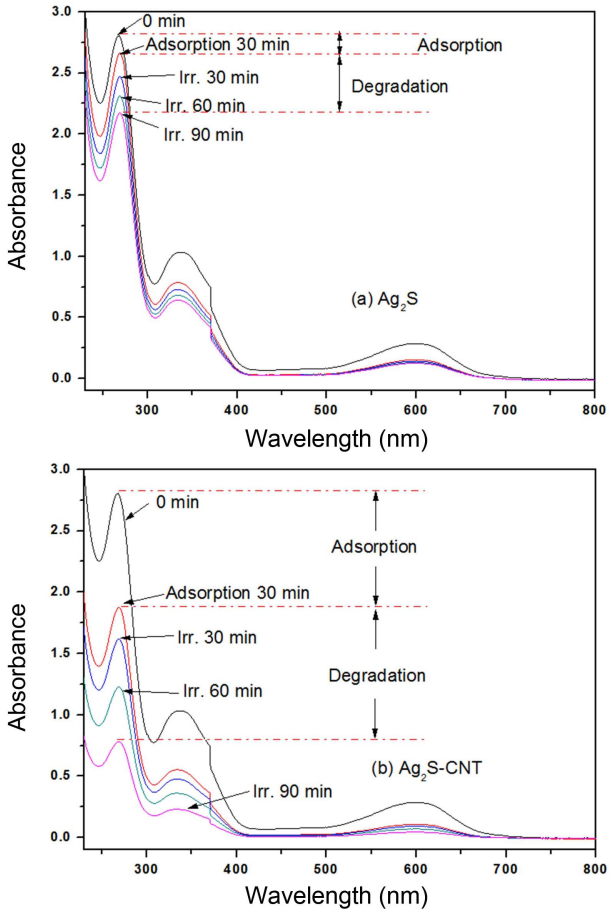

Fig. 6. Degradation of TBA under visible light.

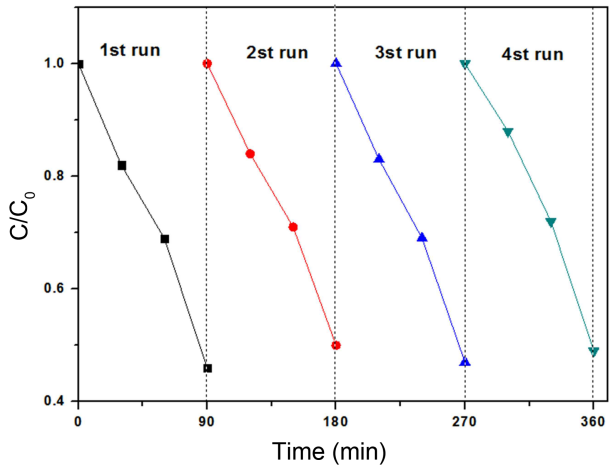

Fig. 7. Cycling runs about the photocatalytic degradation of TBA with sample under visible light irradiation.

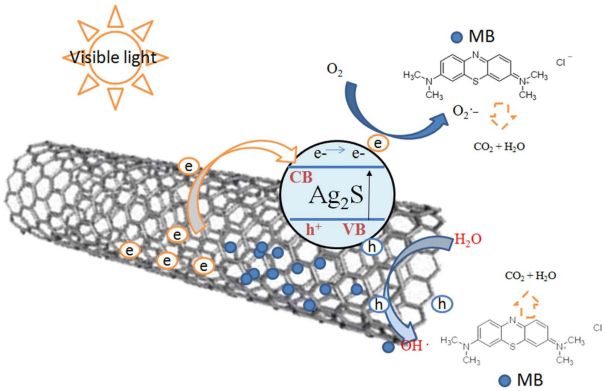

Fig. 8. Schematic diagram of the catalyst growth machanism, separation of photogenerated electrons and holes on the Ag_2S-CNT interface.

decrease in concentration was evaluated at the λ_{max} values of the dyes; which were determined from the absorption spectra of the dyes. However, due to confidential issues of the manufacturing company, detailed information about the TBA of textile dyes was not found. However, UV/Vis-light spectroscopic analysis and the rate determination of the drastic decline in the dye concentration clearly indicated photo-catalysis.

In order to further demonstrate the photo-stability and cyclic performance of the Ag_2S-CNT composite photo-catalyst, cycle experimental in the photo-catalytic degradation of TBA in the presence of Ag_2S-CNT under visible light were conducted. As shown in Fig. 7, the photo-catalysts did not exhibit any significant loss of photo-catalytic activity after four runs of TBA degradation, which indicates that the Ag_2S-CNT photo-catalyst has high stability and cannot be photo-corroded during the photo-catalytic oxidation of the TBA molecules. Thus, the Ag_2S-CNT composite photo-catalyst is promising for practical applications in environmental purification. CNT modification can not only improve photo-catalytic performance but also long-term stability of the Ag_2S nano-crystals. This result is significant from the viewpoint of practical application, as the enhanced photo-catalytic activity and prevention of catalyst deactivation will lead to more cost-effective operation.[18)]

Ag_2S has a relativity narrow band-gap and can be used to induce photo-catalysis with visible light irradiation. We propose that the hydroxyl radical on the surface of nanoparticle Ag_2S was easily generated. This means that organic pollutants, which have already been adsorbed on the photo-catalysts, may be degraded due to the appearance of a hydroxyl radical, resulting in the enhancement of photo-degradation performance.[19)]

In the CNT modified Ag_2S system, CNTs act as electron sensitizers and donators in the composite. They may accept the electrons photo-induced by light irradiation. It is considered that photo-induced charge-transfer occurs during the electronic interaction between the carbon layers (or walls) of the CNTs and the Ag_2S. The electrons on the surface of CNTs migrate to the surface of the Ag_2S and thus lead to a higher rate of reduction in the e^-/h^+ pair recombination. Thus CNT modified Ag_2S can increase of photon efficiency, which reduces the quantum yield of the Ag_2S catalyst. Ag_2S also can enhance the adsorption effect during discoloration processes.[20,21)] Figure 8 shows a schematic diagram of the

catalyst growth mechanism, separation of photo-generated electrons, and holes on the Ag_2S-CNT interface.

4. Conclusion

In this study, the photo-catalytic properties of Ag_2S-CNT composites were investigated. The XRD results indicated that the phase type was acanthite Ag_2S phase. The FT-IR results showed that the Ag_2S-band transfers electrons to CNT with functional groups attached. The adsorption and surface properties, as structural and chemical composition of the Ag_2S-CNT composites, were investigated. In comparison with the separate effects of Ag_2S and CNT nanoparticles, the photo-chemical effect of the CNT photosensitized-Ag_2S composites increased significantly due to the synergistic effect between the CNT and Ag_2S nanoparticles.

REFERENCES

1. O. K. Dalrymple, E. Stefanakos, M. A. Trotz, and D. Y. Goswami, "A Review of the Mechanisms and Modeling of Photocatalytic Disinfection," *Appl. Catal. B*, **98** [1-2] 27-38 (2010).
2. P. Xu, T. Xu, J. Lu, S. M. Gao, N. S. Hosmane, B. B. Huang, Y. Dai, and Y. B. Wang, "Visiblelight-driven Photocatalytic S- and C-codoped Meso/Nanoporous TiO_2," *Energy Environ. Sci.*, **3** [8] 1128-34 (2010).
3. S. Bagwasi, B. Z. Tian, J. L. Zhang, and M. Nasir, "Synthesis, Characterization and Application of Bismuth and Boron Co-doped TiO_2: A Visible Light Active Photocatalyst," *Chem. Eng. J.*, **217** 108-18 (2013).
4. L. Zhu, Z. D. Meng, and W. C. Oh, "Facile Synthesis, Characterization and Photocatalytic Activity of MWCNT-supported Metal Sulfide Composites under Visible Light Irradiation," *J. Kor. Ceram. Soc.*, **49** [2] 155-60 (2012).
5. D. Wang, C. Hao, W. Zheng, Q. Peng, T. Wang, Z. Liao, D. Yu, and Y. Li, "Ultralong Single-crystalline Ag_2S Nanowires: Promising Candidates for Photoswitches and Room-temperature Oxygen Sensors," *Adv. Mater.*, **20** [13] 2628-32 (2008).
6. E. S. Lee, K. M. Lee, S. I. Yoon, Y. G. Ko, and D. H. Shin, "Influence of CNT Incorporation on the Photovoltaic Behavior of TiO_2 Films Formed by High-voltage Electrophoretic Deposition," *Curr. Appl. Phys.*, **13** [2] 26-29 (2013).
7. H. J. Choi, J. E. Shin, G. W. Lee, N. G. Park, K. Kim, and S. C. Hong, "Effect of Surface Modification of Multi-walled Carbon Nanotubes on the Fabrication and Performance of Carbon Nanotube based Counter Electrodes for Dye-sensitized Solar Cells," *Curr. Appl. Phys.*, **10** [2] S165-67 (2010).
8. G. Jiang, L. Wang, C. Chen, X. Dong, T. Chen, and H. Yu, "Attachment of Branched Molecules on Multiwalled Carbon Nano- tubes," *Mater Lett.*, **59** [16] 2085–89 (2005).
9. H. Dong and K. Lu, "Attaching Titania Nanoparticles onto Shortened Carbon Nanotubes by Electrostatic Attraction," *Int. J. Appl. Ceram. Technol.*, **6** [2] 216–22 (2009).
10. X. W. Zhang, M. H. Zhou, and L. C. Lei, "Preparation of Photocatalytic TiO_2 Coating of Nanosized Particles Supported on Activated Carbon by AP-MOCVD," *Carbon*, **43** [8] 1700-08 (2005).
11. Z. D. Meng, T. Ghosh, L. Zhu, J. G. Choi, C. Y. Park, and W. C. Oh, "Synthesis of Fullerene Modified with Ag_2S with High Photocatalytic Activity under Visible Light," *J. Mater. Chem.*, **22** [31] 16127-35 (2012).
12. W. Han and A. Zettl, "Coating Single-walled Carbon Nanotubes with Tin Oxide," *Nano Lett.*, **3** [5] 681–83 (2003).
13. Z. D. Meng, M. M. Peng, L. Zhu, and W. C. Oh, "Fullerene Modification CdS/TiO_2 to Enhancement Surface Area and Modification of Photocatalytic Activity under Visible Light," *Appl. Catal. B*, **113-114** 141-49 (2012).
14. Y. Du, B. Xu, T. Fu, M. Cai, F. Li, Y. Zhang, and Q. Wang, "Near-infrared Photoluminescent Ag_2S Quantum Dots from a Single Source Precursor," *J. Am. Chem. Soc.*, **132** [5] 1470 (2010).
15. K. Nagasuna, T. Akita, M. Fujishima, and H. Tada, "Photodeposition of Ag_2S Quantum Dots and Application to Photoelectrochemical Cells for Hydrogen Production under Simulated Sunlight," *Langmuir*, **27** [11] 7294-300 (2011).
16 K. Hernadi, E. Couteau, J. W. Seo, and L. Forro, "$Al(OH)_3$/multiwalled Carbon Nanotube Composite: Homogeneous Coverage of $Al(OH)_3$ on Carbon Nanotube Surfaces," *Langmuir*, **19** [17] 7026-29 (2003).
17. M. D. Donohue and G. L. Aranovich, "A New Classification of Isotherms for Gibbs Adsorption of Gases on Solids," *Fluid Phase Equilib.*, **158-160** 557-63 (1999).
18. Z. D. Meng, L. Zhu, J. G. Choi, C. Y. Park, and W. C. Oh, "Preparation, Characterization and Photocatalytic Behavior of WO_3-fullerene/TiO_2 Catalysts under Visible Light," *Nanoscale Res. Lett.*, **6** [1] 459 (2011).
19. Y. Xie, S. H. Heo, Y. N. Kim, S. H. Yoo, and S. O. Cho, "Synthesis and Visible-light-induced Catalytic Activity of Ag_2S-coupled TiO_2 Nanoparticles and Nanowires, " *Nanotechnology*, **21** [1] 015703 (2010).
20. P. Peng, B. Sadtler, A. P. Alivisatos, and R. J. Saykally, "Exciton Dynamics in CdS-Ag_2S Nanorods with Tunable Composition Probed by Ultrafast Transient Absorption Spectroscopy," *J. Phys. Chem. C*, **114** [13] 5879-85 (2010).
21. D. Baowan, W. Triampo, and D. Triampo, "Encapsulation of TiO_2 Nanoparticles into Single-walled Carbon Nanotubes," *New J. Phys.*, **11** 093011 (2009).